JOURNAL OF GUIDANCE, CONTROL, AND DYNAMICS
Vol. 22, No. 2, March–April 1999

Adaptive Control of Electrically Driven Space Robots Based on Virtual Decomposition

Wen-Hong Zhu and Joris De Schutter
Katholieke Universiteit Leuven, B-3001 Leuven, Belgium

A systematic approach named virtual decomposition is presented for adaptive control of space robots incorporating motor dynamics. Virtual decomposition imposes a modular structure on both control design and stability analysis. In the control design, the control problem of the complete system is converted into the control problem of each subsystem (rigid body or joint), whereas the nonholonomic constraints are represented by a set of constraint equations imposed on the required acceleration. Two alternative joint control modes, namely, motor current control and motor voltage control, are considered. Parameter adaptation can be carried out independently for each subsystem, which makes decentralized parameter adaptation possible. In the stability analysis, each subsystem (rigid body or joint) is assigned a nonnegative accompanying function. The dynamic interaction between every two physically connected subsystems is completely represented by a virtual power flow through their connection. The system Lyapunov function is formed by merely adding all nonnegative accompanying functions assigned to the subsystems. Lyapunov stability is ensured and computer simulations are conducted. The proposed approach is a general one that can be extended to treat a variety of space robotic systems due to its modular structure.

I. Introduction

SPACE robots are essentially multibody systems with underactuation.[1,2] The particular problem of space robots is how to handle the dynamic coupling between the robot manipulator and the base (a satellite or a shuttle) because the motion of the base will affect the motion of the manipulator and vice versa. Roughly speaking, space robots can be classified into three categories[3,4]: 1) free floating, where neither the position nor the orientation of the base is controlled for the purpose of energy saving; 2) free flying, where only the orientation of the base is controlled through reaction wheels for the purpose of keeping a communication link with the ground and generating electrical power from the solar panels; and 3) full controlling, where both the position and the orientation of the base are controlled through jet thrusts and reaction wheels to compensate for large external disturbances. For the third category, the space robot can be treated as a special redundant manipulator.[5,6] However, for the first two categories, the number of actuators is less than the degrees of freedom (DOF). This underactuation imposes nonholonomic constraints on the space robotic systems.[7] Egeland and Sagli[5] addressed motion decoupling between the end-effector and the base by using resolved acceleration control and recursive calculation of kinematics and dynamics. Papadopoulos and Dubowsky[8] studied the similarity between articulated manipulators and space robots and suggested that nearly any control algorithm used for articulated manipulators can be employed in the control of space robots, provided that dynamic singularity[9] is avoided. With respect to the so-called resolved rate control, a very useful method in practical applications, the concept of a generalized Jacobian matrix was proposed by Umetani and Yoshida.[10] A relative kinematic control approach was also developed. Oda[11] proposed a coordinated control scheme in which both the base (satellite) and the manipulator have their own controllers. A feedforward signal is sent to the base controller to compensate for the momentum imposed by the motion of the manipulator. From a point of view of underactuated systems, Jain and Rodriguez[12] presented a general approach for recursive calculation of both forward and inverse kinematics and dynamics.

Wen-Hong Zhu was born in Nanjing, China, in 1963. He received his B.S. and M. S. degrees, both in aeronautical control engineering, from Northwestern Polytechnical University, Xi'an, China, in 1984 and 1987, respectively. He received his Ph.D. degree in information and control engineering from Xi'an Jiaotong University, Xi'an, China, in 1991. He was employed by the CIET, KAIST, Korea, as a Postdoctoral Fellow in 1995. From 1996 to 1997, he was awarded a Postdoctoral Fellowship by the Katholieke Universiteit Leuven, Belgium. He is currently a Postdoctoral Fellow with Prof. Tim Salcudean in the Department of Electrical and Computer Engineering at the University of British Columbia, Canada. His research interests include stability guaranteed teleoperation, teleoperated control of medical robots, adaptive control of space robots, adaptive control of robots with rigid/flexible joints, coordinated control of multiarm robots, variable structure control of robots with only joint position measurements, and the application of robots in service fields.

Joris De Schutter received his B.E. and Ph.D. degrees in mechanical engineering from the Katholieke Universiteit Leuven, Belgium, in 1980 and 1986, respectively, and his M.S. degree from the Massachusetts Institute of Technology in 1981. He then worked as a control systems engineer in industry. In 1986 he became a Lecturer with the Department of Mechanical Engineering, the Production Engineering, Machine Design, and Automation Division, at the Katholieke Universiteit Leuven, where he has been a full professor since 1995. He teaches courses in kinematics and dynamics of machinery, control, and robotics and is the coordinator of the study program in mechatronics. He has published papers on sensor-based robot control (especially force control), position control of flexible systems and drive systems, and robot programming.

Received Aug. 26, 1996; revision received Aug. 10, 1998; accepted for publication Sept. 2, 1998.

Control and simulation of multiarm space robots was investigated by Yoshida et al.,[13] Yokokohji et al.,[14] Murphy et al.,[15] and Miles and Cannon.[16] In these approaches, dynamic interactions between the base and the multimanipulator are considered, and recursive calculations are provided. Coordinated control of two space robots capturing a common object was studied by Zhu et al.[17] and Dickson and Cannon.[18]

All approaches just mentioned are based on the assumption of exact dynamic parameters. This assumption is sometimes impracticable because of unprecisely known fuel consumption and operations with unknown payloads, such as when capturing a satellite. This motivates development of adaptive control.[19−27] The nonholonomic constraints imposed on space robotic systems make adaptive control design a very challenging problem. Walker and Wee[19] proposed a Lagrangian-model-based adaptive control approach capable of treating parameter uncertainties by using joint acceleration measurements. Xu et al.[20,21] pointed out that linear parameterization can be done only in joint space but not in Cartesian space. Gu and Xu[22] proposed an augmentation approach described in Cartesian space with complete base acceleration measurements. Chen and Cannon[23] and Ma and Huo[24] proposed approaches specified in Cartesian space and controlled in joint space. Jean and Fu[25] and Shin et al.[26] discussed adaptive robust control of space robots subject to bounded uncertainties. Note that all of these approaches are based on a Lagrangian model, which results in heavy computation. Meanwhile, most approaches[19,22,24] require acceleration measurements. With respect to these drawbacks, Wee et al.[27] recently proposed an adaptive control approach based on an articulated-body model, which does not require acceleration measurements. However, this approach can deal with parameter uncertainty in only one object (the end-effector).

In this paper, adaptive control of space robots is further generalized and simplified by using a systematic approach named virtual decomposition. The control design of the complete system is converted into the control design of each subsystem, namely, rigid body or joint, whereas the dynamic interactions between the subsystems are completely represented by virtual power flows (VPFs). Only the dynamics of the individual rigid bodies and joints, instead of the dynamics of the complete system, are required in the control design. Compared with previous approaches, some features can be summarized as follows. 1) Computation is cheap because the simple dynamics of each subsystem (rigid body or joint) are used, while preserving the full dynamic properties of the system without any model reduction. Compared with Ref. 27, dynamics of a rigid body can be considered as the simplest form of an articulated-body model. 2) The modular control structure allows us to take the motor dynamics into account[28−31] because adaptive control of each joint can be performed independently from adaptive control of rigid bodies. 3) No joint acceleration measurement is required. 4) Parameter adaptation can be carried out independently.

In this paper, free-flying space robots with orientation control are studied first. Then this approach is applied to free-floating space robots. Possible extensions to more complicated space robots are discussed. Finally, a simulation case study is conducted.

II. Kinematics Description

A typical single-arm space robot is illustrated in Fig. 1. This is a six-joint manipulator mounted on a base (satellite or shuttle) that contains three reaction wheels. This system has 15 DOF (6 for the manipulator, 6 for the base, and 3 for the reaction wheels). However, only nine of them can be position/orientation controlled; the remaining six DOF are used to deal with the nonholonomic constraints.

The six joints of the manipulator are numbered sequentially from 1 to 6, whereas the three joints of the reaction wheels are numbered from 7 to 9. The links are numbered in such a way that joint j connects link j with link $j-1$ for $j = 2, \ldots, 6$ and connects link j with the base for $j = 1, 7, 8, 9$. Several coordinate frames are defined as follows. Frame B is fixed to the base to represent the base motion. Frame E is fixed to link 6 (the payload is included in link 6) to characterize the motion of the end-effector. Frame L_j, $j = 1, 2, \ldots, 9$, is fixed to link j with its z axis coincident with the jth joint axis. Frame T_j is fixed to link $j-1$ for $j = 2, \ldots, 6$ and fixed to the base for $j = 1, 7, 8, 9$, with its z axis coincident with the jth joint axis.

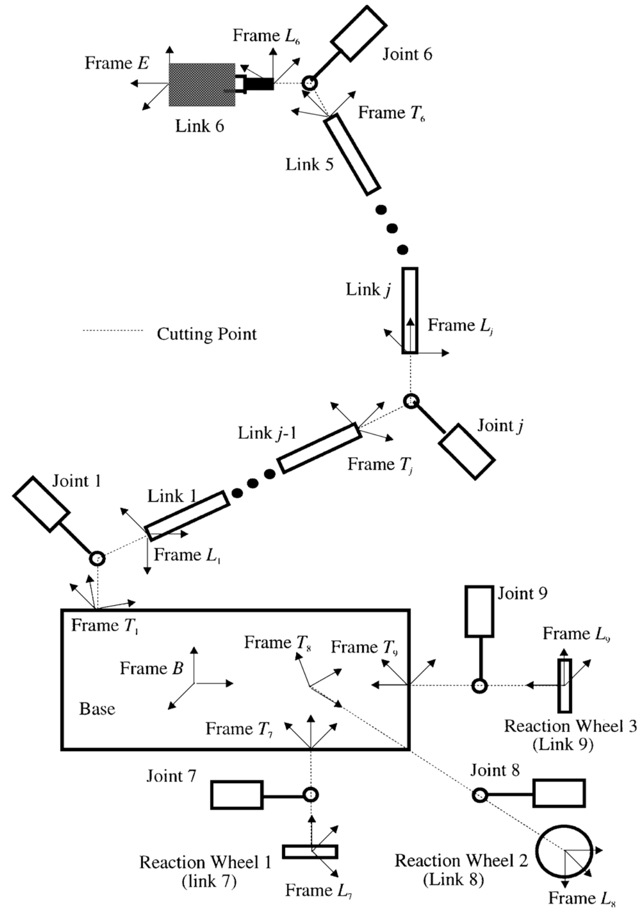

Fig. 1 Space robot with reaction wheels.

Linear and angular velocities and force/moments are all expressed in the corresponding moving frames instead of the inertial frame I to allow easy transformation. We denote

$$^{\alpha}X = [^{\alpha}\nu^T, {}^{\alpha}\omega^T]^T = \left[\left(^{\alpha}R_I \cdot \nu_\alpha\right)^T, \left(^{\alpha}R_I \cdot \omega_\alpha\right)^T\right]^T \in R^6$$

as a generalized linear/angular velocity of moving frame α, expressed in frame α. The terms $^{\alpha}\nu \in R^3$ and $^{\alpha}\omega \in R^3$ denote the linear and angular velocities of frame α and expressed in frame α, respectively, whereas $\nu_\alpha \in R^3$ and $\omega_\alpha \in R^3$ denote the linear and angular velocities of frame α expressed in the inertial frame I. The term $^{\alpha}R_I \in R^{3\times 3}$ denotes an orthogonal rotation transformation matrix that transforms a 3×1 vector expressed in the inertial frame I to that expressed in moving frame α. Obviously, we have

$$\frac{\mathrm{d}}{\mathrm{dt}}\left(^{I}R_\alpha\right) = (\omega_\alpha \times)\left(^{I}R_\alpha\right) \tag{1}$$

where $\times$ denotes the cross product.

Meanwhile, we denote

$$^{\alpha}F = [^{\alpha}f^T, {}^{\alpha}m^T]^T = \left[\left(^{\alpha}R_I \cdot f_\alpha\right)^T, \left(^{\alpha}R_I \cdot m_\alpha\right)^T\right]^T \in R^6$$

as a generalized exerting force/moment measured and expressed in moving frame α. The terms $^{\alpha}f \in R^3$ and $^{\alpha}m \in R^3$ denote the exerting force and moment measured and expressed in moving frame α, respectively, whereas $f_\alpha \in R^3$ and $m_\alpha \in R^3$ denote the exerting force and moment measured in frame α and expressed in the inertial frame I.

Transformation of generalized velocities and forces between two moving frames α and β that are fixed to a common rigid body can be expressed as

$$^{\beta}X = {}^{\alpha}U_\beta^T \cdot {}^{\alpha}X \tag{2}$$

$$^{\beta}F = {}^{\beta}U_\alpha \cdot {}^{\alpha}F \tag{3}$$

where ${}^{\beta}U_{\alpha}$, defined as

$$ {}^{\beta}U_{\alpha} = \begin{bmatrix} {}^{\beta}R_{\alpha} & 0 \\ \left({}^{\beta}r_{\alpha}\times\right)\cdot{}^{\beta}R_{\alpha} & {}^{\beta}R_{\alpha} \end{bmatrix} \in R^{6\times 6} $$

denotes a generalized force/moment transformation matrix that transforms a 6×1 force/moment measured and expressed in frame α to that measured and expressed in frame β. The term ${}^{\beta}r_{\alpha}$ denotes a 3×1 vector pointing from the origin of frame β toward the origin of frame α and expressed in frame β. The term ${}^{\beta}R_{\alpha} \in R^{3\times 3}$ has the same definition as ${}^{I}R_{\alpha}$ except that β is substituted for I.

The velocity of the jth one-dimensional joint is represented by

$$ Z_j \cdot \dot{q}_j = {}^{L_j}X - {}^{T_j}U^{T}_{L_j} \cdot {}^{T_j}X \tag{4} $$

where $\dot{q}_j \in R$ denotes the velocity of the jth joint. The term $Z_j = [0\ 0\ 1\ 0\ 0\ 0]^T$ for a prismatic joint and $Z_j = [0\ 0\ 0\ 0\ 0\ 1]^T$ for a revolute joint, $j = 1, 2, \ldots, 9$.

In view of Eqs. (2) and (4), the extended velocities of the space robot are written as

$$ \mathcal{X} = \mathcal{T} \cdot \begin{bmatrix} \dot{q} \\ {}^{B}X \end{bmatrix} \tag{5} $$

where $\dot{q} = [\dot{q}_1, \ldots, \dot{q}_j, \ldots, \dot{q}_9]^T \in R^9$, whereas

$$ \mathcal{X} = [\dot{q}^T, {}^{B}X^T, {}^{L_1}X^T, \ldots, {}^{L_j}X^T, \ldots, {}^{L_9}X^T]^T \in R^{(9+6+9\times 6)} $$

$$ \mathcal{T} = $$

$$ \begin{bmatrix} & & & I_{(9+6)} & & & & \\ Z_1 & 0 & \ldots & \ldots & \ldots & \ldots & 0 & {}^{B}U^T_{L_1} \\ {}^{L_1}U^T_{L_2}\cdot Z_1 & Z_2 & 0 & & & & 0 & {}^{B}U^T_{L_2} \\ \vdots & \vdots & \ddots & \ddots & & & \vdots & \vdots \\ {}^{L_1}U^T_{L_6}\cdot Z_1 & {}^{L_2}U^T_{L_6}\cdot Z_2 & \ldots & Z_6 & 0 & 0 & 0 & {}^{B}U^T_{L_6} \\ 0 & 0 & \ldots & 0 & Z_7 & 0 & 0 & {}^{B}U^T_{L_7} \\ 0 & 0 & \ldots & 0 & 0 & Z_8 & 0 & {}^{B}U^T_{L_8} \\ 0 & 0 & \ldots & 0 & 0 & 0 & Z_9 & {}^{B}U^T_{L_9} \end{bmatrix} $$

$$ \in R^{69\times 15} $$

and I_n is a n-dimensional identity matrix.

The term $[\dot{q}^T\ \ {}^{B}X^T]^T \in R^{15}$ denotes the independent velocities of the space robot. However, only nine DOF are subject to the control specifications, whereas the remaining six DOF are subject to the nonholonomic constraints. It follows that

$$ \begin{bmatrix} \dot{q} \\ {}^{B}X \end{bmatrix} = \begin{bmatrix} \dot{q}_m \\ \dot{q}_w \\ {}^{B}\nu \\ {}^{B}\omega \end{bmatrix} = \begin{bmatrix} I_6 & 0 \\ 0 & 0 \\ 0 & 0 \\ 0 & I_3 \end{bmatrix} \cdot \begin{bmatrix} \dot{q}_m \\ {}^{B}\omega \end{bmatrix} + \begin{bmatrix} 0 & 0 \\ I_3 & 0 \\ 0 & I_3 \\ 0 & 0 \end{bmatrix} \cdot \begin{bmatrix} \dot{q}_w \\ {}^{B}\nu \end{bmatrix} \tag{6} $$

for joint space specification, or alternately

$$ \begin{bmatrix} \dot{q} \\ {}^{B}X \end{bmatrix} = \begin{bmatrix} J^{-1}\cdot{}^{E}U^T_{L_6} & 0 & -J^{-1}\cdot{}^{B}U^T_{L_6} \\ 0 & I_3 & 0 \\ 0 & 0 & I_6 \end{bmatrix} $$

$$ \times \left(\begin{bmatrix} I_6 & 0 \\ 0 & 0 \\ 0 & 0 \\ 0 & I_3 \end{bmatrix} \cdot \begin{bmatrix} {}^{E}X \\ {}^{B}\omega \end{bmatrix} + \begin{bmatrix} 0 & 0 \\ I_3 & 0 \\ 0 & I_3 \\ 0 & 0 \end{bmatrix} \cdot \begin{bmatrix} \dot{q}_w \\ {}^{B}\nu \end{bmatrix} \right) \tag{7} $$

for Cartesian space specification, where $\dot{q}_m = [\dot{q}_1, \ldots, \dot{q}_j, \ldots, \dot{q}_6]^T \in R^6$, $\dot{q}_w = [\dot{q}_7\ \ \dot{q}_8\ \ \dot{q}_9]^T \in R^3$, and

$$ J = \left[{}^{L_1}U^T_{L_6}\cdot Z_1 \quad {}^{L_2}U^T_{L_6}\cdot Z_2 \quad \cdots \quad Z_6 \right] \in R^{6\times 6} $$

is the Jacobian matrix of the manipulator. The term $[\dot{q}_w^T\ \ {}^{B}\nu^T]^T \in R^6$ denotes the independent velocities associated with the nonholonomic constraints, whereas $[\dot{q}_m^T\ \ {}^{B}\omega^T]^T \in R^9$ or $[{}^{E}X^T\ \ {}^{B}\omega^T]^T \in R^9$ denote the independent velocities associated with the control specifications, which are described next.

III. Control Specifications

Two alternative control specifications are 1) the joint space specification ($\sigma = 1$), the orientation of the base and the six joint positions of the manipulator, or 2) the Cartesian space specification ($\sigma = 0$), the orientation of the base and the position/orientation of frame E.

Symbol σ is used to distinguish between the joint space specification and the Cartesian space specification.

In the case of the joint space specification ($\sigma = 1$), a reference frame B_d is defined. The reference frame B_d and frame B have a common origin but different orientation. For each joint q_j, $j = 1, 2, \ldots, 6$, the reference signal q_{jd} is also given. The control objective is to make the frame B track the orientation of its reference frame B_d and to make q_j track its reference signal q_{jd}, $j = 1, 2, \ldots, 6$. Therefore, the required velocities are designed as

$$ \begin{bmatrix} \dot{q}_{mr} \\ {}^{B}\omega_r \end{bmatrix} = \begin{bmatrix} \dot{q}_{md} \\ {}^{B}R_I \cdot \omega_{B_d} \end{bmatrix} + \lambda \cdot \begin{bmatrix} q_{md} - q_m \\ {}^{B}\mu \end{bmatrix} \tag{8} $$

where subscript r refers to the corresponding required vector; $\lambda > 0$. The term $q_{md} = [q_{1d}, \ldots, q_{jd}, \ldots, q_{6d}]^T \in R^6$ denotes the reference joint positions. The term ${}^{B}\mu \in R^3$ is the vector part of a four-parameter unit quaternion called Euler parameter $[\xi_B, {}^{B}\mu^T]^T \in R^4$, defined as

$$ \xi_B = \cos(\phi_B/2), \qquad {}^{B}\mu = \sin(\phi_B/2)\cdot{}^{B}k $$

where ${}^{B}k$ denotes a unit vector $\boldsymbol{k}_B$ expressed in frame B. The pair $(\phi_B, \boldsymbol{k}_B)$ is determined in such a way that rotating frame B about $\boldsymbol{k}_B$ through ϕ_B yields frame B_d. An approach for calculating $[\xi_B,\ {}^{B}\mu^T]^T$ from a given ${}^{B}R_{B_d}$ is proposed by Klumpp.[32] The derivative of $[\xi_B,\ {}^{B}\mu^T]^T$ can be found in Ref. 33 as

$$ \begin{aligned} \dot{\xi}_B &= -\tfrac{1}{2}\cdot{}^{B}\Delta\omega^T\cdot{}^{B}\mu \\ \frac{\mathrm{d}}{\mathrm{d}t}({}^{B}\mu) &= \tfrac{1}{2}\left[\xi_B\cdot{}^{B}\Delta\omega + ({}^{B}\Delta\omega\times)\cdot{}^{B}\mu\right] \end{aligned} \tag{9} $$

where ${}^{B}\Delta\omega = {}^{B}R_I\cdot(\omega_{B_d} - \omega_B)$ denotes the angular velocity error expressed in frame B.

In the case of the Cartesian space specification ($\sigma = 0$), the reference frame B_d remains the same. A new reference frame E_d is defined to replace the reference joint positions q_{md}. The control objective is to make frame E track its reference frame E_d and to make frame B track the orientation of its reference frame B_d. The corresponding required velocities are designed as

$$ \begin{bmatrix} {}^{E}X_r \\ {}^{B}\omega_r \end{bmatrix} = \mathrm{diag}\left\{{}^{E}R_I, {}^{E}R_I, {}^{B}R_I\right\}\cdot\begin{bmatrix} \nu_{E_d} \\ \omega_{E_d} \\ \omega_{B_d} \end{bmatrix} + \lambda\cdot\begin{bmatrix} {}^{E}e \\ {}^{E}\mu \\ {}^{B}\mu \end{bmatrix} \tag{10} $$

where ${}^{E}e \in R^3$ denotes a position error vector pointing from the origin of frame E toward the origin of frame E_d and expressed in frame E. The term ${}^{E}\mu \in R^3$ has a similar definition as ${}^{B}\mu \in R^3$ except that E is substituted for B and E_d is substituted for B_d. Some literature related to path planning[34–36] can be applied here to generate desired trajectories subject to various optimizations. However, in the case of the Cartesian space specification, the dynamic singularity problem[9] should be considered.

According to Eq. (5), we have

$$ \mathcal{X}_r = \mathcal{T}\cdot\begin{bmatrix} \dot{q}_r \\ {}^{B}X_r \end{bmatrix} \tag{11} $$

where $\mathcal{X}_r$ denotes the required vector of $\mathcal{X}$ defined by Eq. (5). The term $[\dot{q}_r^T\ \ {}^{B}X_r^T]^T$ is obtained either from Eq. (6) by replacing $[\dot{q}^T\ \ {}^{B}X^T]^T$ with $[\dot{q}_r^T\ \ {}^{B}X_r^T]^T$, $[\dot{q}_m^T\ \ {}^{B}\omega^T]^T$ with $[\dot{q}_{mr}^T\ \ {}^{B}\omega_r^T]^T$, and $[\dot{q}_w^T\ \ {}^{B}\nu^T]^T$ with $[\dot{q}_{wr}^T\ \ {}^{B}\nu_r^T]^T$, if the joint control specification is chosen, or from Eq. (7) by replacing $[\dot{q}^T\ \ {}^{B}X^T]^T$ with $[\dot{q}_r^T\ \ {}^{B}X_r^T]^T$,

$[{}^E X^T\ \ {}^B\omega^T]^T$ with $[{}^E X_r^T\ \ {}^B\omega_r^T]^T$, and $[\dot{q}_w^T\ \ {}^B\nu^T]^T$ with $[\dot{q}_{wr}^T\ \ {}^B\nu_r^T]^T$, if the Cartesian control specification is chosen.

In view of Eqs. (6), (7), (8), and (10), differentiating Eq. (11) gives

$$\dot{\mathcal{X}}_r = \mathcal{T}\cdot\frac{\mathrm{d}}{\mathrm{d}t}\begin{bmatrix}\dot{q}_r\\ {}^B X_r\end{bmatrix} + \dot{\mathcal{T}}\cdot\begin{bmatrix}\dot{q}_r\\ {}^B X_r\end{bmatrix} = \mathcal{A}_x\cdot\begin{bmatrix}\ddot{q}_{wr}\\ \frac{\mathrm{d}}{\mathrm{d}t}\left({}^B\nu_r\right)\end{bmatrix} + \mathcal{B}_x \tag{12}$$

where $\mathcal{A}_x$ and $\mathcal{B}_x$ are a known matrix and a known vector, respectively, because either $(\mathrm{d}/\mathrm{d}t)[\dot{q}_{mr}^T\ \ {}^B\omega_r^T]^T$ or $(\mathrm{d}/\mathrm{d}t)[{}^E X_r^T\ \ {}^B\omega_r^T]^T$, which is used to generate $(\mathrm{d}/\mathrm{d}t)[\dot{q}_r^T\ \ {}^B X_r^T]^T$, is obtained from the derivative of Eq. (8) or the derivative of Eq. (10). Equation (12) indicates that $\dot{\mathcal{X}}_r$ is a linear function of $[\ddot{q}_{wr}^T\ \ (\mathrm{d}/\mathrm{d}t)({}^B\nu_r)^T]^T$, which will be used to handle the nonholonomic constraints imposed on the system, whereas $[\dot{q}_{wr}^T\ \ {}^B\nu_r^T]^T$ can be obtained through integrating $[\ddot{q}_{wr}^T\ \ (\mathrm{d}/\mathrm{d}t)({}^B\nu_r)^T]^T$.

IV. Dynamics and Control of Rigid Bodies

Following the virtual decomposition, the space robot system is virtually decomposed into 9 actuated joints and 10 rigid bodies: 6 links (the payload is considered as a portion of the sixth link), 3 reaction wheels, and the base. Therefore, there are a total of 18 cutting points corresponding to the 18 origins of frames L_j, T_j, $j = 1, 2, \ldots, 9$.

The dynamic equation of a rigid body expressed in the body attached frame α, $\alpha \in \{B, L_1, \ldots, L_j, \ldots, L_9\}$, can be written as

$$M_\alpha\cdot\frac{\mathrm{d}}{\mathrm{d}t}({}^\alpha X) + C_\alpha({}^\alpha\omega)\cdot{}^\alpha X = {}^\alpha\underline{F} \tag{13}$$

where ${}^\alpha\underline{F} \in R^6$ denotes the net force/moment applied to the rigid body and expressed in frame α. The term M_α is constant and $C_\alpha({}^\alpha\omega)$ is skew symmetric. The detailed forms can be found in Ref. 37.

The left-hand side of Eq. (13) can be represented by an expression that is linear in the parameters:

$$M_\alpha\cdot\frac{\mathrm{d}}{\mathrm{d}t}({}^\alpha X) + C_\alpha({}^\alpha\omega)\cdot{}^\alpha X = Y_\alpha^K\cdot\theta_\alpha^K + Y_\alpha\cdot\theta_\alpha$$

where θ_α^K and θ_α denote the known and unknown parameter vectors of the rigid body. The terms Y_α^K and Y_α are the corresponding regressor matrices.

In the adaptive control design, the required net force/moment of the rigid body is designed as

$$\begin{gathered}{}^\alpha\underline{F}_r = Y_{\alpha r}^K\cdot\theta_\alpha^K + Y_{\alpha r}\cdot\hat{\theta}_\alpha + K_\alpha\cdot\left({}^\alpha X_r - {}^\alpha X\right) + P_\alpha\\ Y_{\alpha r}^K\cdot\theta_\alpha^K + Y_{\alpha r}\cdot\theta_\alpha = M_\alpha\cdot\frac{\mathrm{d}}{\mathrm{d}t}\left({}^\alpha X_r\right) + C_\alpha({}^\alpha\omega)\cdot{}^\alpha X_r\\ P_\alpha = \begin{cases}\begin{bmatrix}0\\ k_B\cdot{}^B\mu\end{bmatrix} & \alpha = B\\ {}^{L_6}U_E\cdot\begin{bmatrix}k_{E1}\cdot{}^E e\\ k_{E2}\cdot{}^E\mu\end{bmatrix} & \{\alpha = L_6\}\ \text{and}\ \{\sigma = 0\}\\ 0 & \text{otherwise}\end{cases}\end{gathered} \tag{14}$$

where $\alpha \in \{B, L_1, \ldots, L_j, \ldots, L_9\}$. The terms $Y_{\alpha r}^K$ and $Y_{\alpha r}$ denote two regressor matrices corresponding to the required vectors. The term K_α is a positive-definite matrix; $k_B > 0$, $k_{E1} > 0$, and $k_{E2} > 0$. The first two terms on the right-hand side of Eq. (14) represent model-based feedforward compensation. The term $\hat{\theta}_\alpha$ denotes the estimate of θ_α. The third and fourth terms on the right-hand side of Eq. (14) represent velocity and position/orientation feedback. The unknown parameters are updated through

$$\begin{gathered}(\dot{\hat{\theta}}_\alpha)_\gamma = \rho_\gamma^\alpha\cdot\kappa_\gamma^\alpha\cdot s_\gamma^\alpha\\ s_\gamma^\alpha = (Y_{\alpha r})_\gamma^T\cdot\left({}^\alpha X_r - {}^\alpha X\right)\\ \kappa_\gamma^\alpha = \begin{cases}0 & (\hat{\theta}_\alpha)_\gamma \le (\theta_\alpha)_\gamma^-\ \text{and}\ s_\gamma^\alpha \le 0\\ 0 & (\hat{\theta}_\alpha)_\gamma \ge (\theta_\alpha)_\gamma^+\ \text{and}\ s_\gamma^\alpha \ge 0\\ 1 & \text{otherwise}\end{cases}\end{gathered} \tag{15}$$

where $\rho_\gamma^\alpha > 0$ denotes the update gain for the γth parameter. The term $(Y_{\alpha r})_\gamma$ denotes the γth column of $Y_{\alpha r}$, and $(\theta_\alpha)_\gamma$ denotes the γth element of θ_α. The terms $(\theta_\alpha)_\gamma^+$ and $(\theta_\alpha)_\gamma^-$ denote the upper and lower bounds of the physical parameter $(\theta_\alpha)_\gamma$. These upper and lower bounds should be known a priori. Equation (15) indicates that each unknown parameter can be updated within its upper and lower bounds independently.

In view of Eqs. (13–15), a nonnegative accompanying function

$$\begin{gathered}V_\alpha = \tfrac{1}{2}\left({}^\alpha X_r - {}^\alpha X\right)^T\cdot M_\alpha\cdot\left({}^\alpha X_r - {}^\alpha X\right) + \tfrac{1}{2}(\theta_\alpha - \hat{\theta}_\alpha)^T\cdot\Gamma_\alpha\cdot(\theta_\alpha - \hat{\theta}_\alpha) + \Psi_\alpha\\ \Psi_\alpha = \begin{cases}k_B\cdot[{}^B\mu^T\cdot{}^B\mu + (1-\xi_B)^2] & \alpha = B\\ \tfrac{1}{2}k_{E1}\cdot{}^E e^T\cdot{}^E e + k_{E2}\cdot\left[{}^E\mu^T\cdot{}^E\mu + (1-\xi_E)^2\right] & \{\alpha = L_6\}\ \text{and}\ \{\sigma = 0\}\\ 0 & \text{otherwise}\end{cases}\end{gathered} \tag{16}$$

is chosen for $\alpha \in \{B, L_1, \ldots, L_j, \ldots, L_9\}$ so that

$$\begin{gathered}\dot{V}_\alpha \le -\left({}^\alpha X_r - {}^\alpha X\right)^T\cdot K_\alpha\cdot\left({}^\alpha X_r - {}^\alpha X\right) - \Upsilon_\alpha + \left({}^\alpha X_r - {}^\alpha X\right)^T\cdot\left({}^\alpha\underline{F}_r - {}^\alpha\underline{F}\right)\\ \Upsilon_\alpha = \begin{cases}\lambda\cdot k_B\cdot{}^B\mu^T\cdot{}^B\mu & \alpha = B\\ \lambda\cdot k_{E1}\cdot{}^E e^T\cdot{}^E e + \lambda\cdot k_{E2}\cdot{}^E\mu^T\cdot{}^E\mu & \{\alpha = L_6\}\ \text{and}\ \{\sigma = 0\}\\ 0 & \text{otherwise}\end{cases}\end{gathered} \tag{17}$$

where $\Gamma_\alpha = \mathrm{diag}\{1/\rho_1^\alpha, \ldots, 1/\rho_\gamma^\alpha, \ldots\}$. The term ξ_E has a similar definition as ξ_B except that E is substituted for B. The procedure for deriving Eq. (17) from Eq. (16) is given in the Appendix.

The last term on the right-hand side of Eq. (17) represents the dynamic interactions between the rigid body and the remaining subsystems.

In view of Fig. 1, the net force/moment ${}^\alpha\underline{F}$ in Eq. (13) can be represented by

$${}^{L_j}\underline{F} = {}^{L_j}F - {}^{L_j}U_{T_{(j+1)}}\cdot{}^{T_{(j+1)}}F; \qquad j = 1, \ldots, 5 \tag{18}$$

$${}^{L_j}\underline{F} = {}^{L_j}F; \qquad j = 6, \ldots, 9 \tag{19}$$

$${}^B\underline{F} = -{}^B U_{T_1}\cdot{}^{T_1}F - \sum_{j=7}^{9}{}^B U_{T_j}\cdot{}^{T_j}F \tag{20}$$

where ${}^{L_j}F \in R^6$ denotes the force/moment exerted by link $j-1$ onto link j for $j = 2, \ldots, 6$, and by the base onto link j for $j = 1, 7, 8, 9$. Obviously, ${}^{T_j}F = {}^{T_j}U_{L_j}\cdot{}^{L_j}F$.

In terms of Eqs. (14) and (18–20), the required force/moment is designed as

$${}^{L_j}F_r = {}^{L_j}\underline{F}_r; \qquad j = 6, \ldots, 9 \tag{21}$$

$${}^{L_j}F_r = {}^{L_j}\underline{F}_r + {}^{L_j}U_{L_{(j+1)}}\cdot{}^{L_{(j+1)}}F_r; \qquad j = 5, \ldots, 1 \tag{22}$$

subject to the constraint

$${}^B\underline{F}_r + {}^B U_{T_1}\cdot{}^{T_1}F_r + \sum_{j=7}^{9}{}^B U_{T_j}\cdot{}^{T_j}F_r = {}^B\underline{F}_r + \sum_{j=1}^{9}{}^B U_{L_j}\cdot{}^{L_j}\underline{F}_r = 0 \tag{23}$$

In view of Eqs. (2), (3), and (18–23) and the fact that ${}^{T_j}F = {}^{T_j}U_{L_j}\cdot{}^{L_j}F$ and ${}^{T_j}F_r = {}^{T_j}U_{L_j}\cdot{}^{L_j}F_r$, $j = 1, 2, \ldots, 9$, it follows that

$$\left({}^{L_j}X_r - {}^{L_j}X\right)^T\cdot\left({}^{L_j}\underline{F}_r - {}^{L_j}\underline{F}\right) = W_{L_j}; \qquad j = 6, \ldots, 9 \tag{24}$$

$$\left({}^{L_j}X_r - {}^{L_j}X\right)^T\cdot\left({}^{L_j}\underline{F}_r - {}^{L_j}\underline{F}\right) = W_{L_j} - W_{T_{(j+1)}} \qquad j = 1, \ldots, 5 \tag{25}$$

$$\left({}^B X_r - {}^B X\right)^T\cdot\left({}^B\underline{F}_r - {}^B\underline{F}\right) = -W_{T_1} - \sum_{j=7}^{9}W_{T_j} \tag{26}$$

where

$$W_\alpha = \left({}^\alpha X_r - {}^\alpha X\right)^T \cdot \left({}^\alpha F_r - {}^\alpha F\right) \tag{27}$$

denotes the VPF (Ref. 37) at frame α.

Equations (24–26) together with Eq. (17) show that the dynamic interactions between a rigid body and the remaining subsystems can be completely represented by the VPFs at the cutting points of the rigid body. The sign of these VPFs depends on the reference direction of each exerting force/moment. These VPFs will be handled in Sec. VI.

The constraint equation (23) completely characterizes the control issue related to the nonholonomic constraints imposed on the space robotic systems. Compared with Ref. 16, the way of dealing with the nonholonomic constraints is very simple because only Eq. (23) is utilized.

V. Dynamics and Control of Joints

In this section we concentrate on independent adaptive control design of the joints. Two alternative modes—motor current control and motor voltage control—are discussed.

Motor Current Control

Motor torque control implies that the motor armature current can be directly applied by the controller. The dynamics of the jth joint including drive mechanism are

$$I_j^* \cdot \ddot{q}_j + d_j \cdot \dot{q}_j = k_j \cdot I_{cj} - Z_j^T \cdot {}^{L_j}F \tag{28}$$

where $j = 1, 2, \ldots, 9$. The term I_j^* is the equivalent rotational inertia of the motor rotor, d_j is the coefficient of viscous friction, k_j denotes the unknown torque/current constant, I_{cj} denotes the motor armature current, and $Z_j^T \cdot {}^{L_j}F$ is the projection of the force/moment onto the joint axis.

The applied armature current is designed as

$$I_{cjd} = \left[Y_{jr} \cdot \hat{\theta}_j + Z_j^T \cdot {}^{L_j}F_r\right] \cdot \hat{\zeta}_j + k_{vj}^* \cdot (\dot{q}_{jr} - \dot{q}_j) + \sigma_j \cdot k_{pj}^* \cdot (q_{jd} - q_j) \tag{29}$$

where

$$Y_{jr} = [\ddot{q}_{jr} \quad \dot{q}_{jr}], \qquad \theta_j = \left[I_j^* \quad d_j\right]^T, \qquad \zeta_j \triangleq 1/k_j$$

$$k_{vj}^* > 0, \qquad k_{pj}^* > 0, \qquad \sigma_j = \begin{cases} \sigma & j = 1, 2, \ldots, 6 \\ 0 & \text{otherwise} \end{cases}$$

and where $\hat{\theta}_j$ and $\hat{\zeta}_j$ are updated through

$$\begin{gathered} (\dot{\hat{\theta}}_j)_\gamma = \rho_{j\gamma} \cdot \kappa_{j\gamma} \cdot s_{j\gamma}; \qquad \gamma = 1, 2 \\ s_{j\gamma} = (Y_{jr})_\gamma^T \cdot (\dot{q}_{jr} - \dot{q}_j) \\ \kappa_{j\gamma} = \begin{cases} 0 & (\hat{\theta}_j)_\gamma \le (\theta_j)_\gamma^- \quad \text{and} \quad s_{j\gamma} \le 0 \\ 0 & (\hat{\theta}_j)_\gamma \ge (\theta_j)_\gamma^+ \quad \text{and} \quad s_{j\gamma} \ge 0 \\ 1 & \text{otherwise} \end{cases} \end{gathered} \tag{30}$$

$$\begin{gathered} \dot{\hat{\zeta}}_j = \rho_j^\zeta \cdot \kappa_j^\zeta \cdot s_j^\zeta \\ s_j^\zeta = \left[Y_{jr} \cdot \hat{\theta}_j + Z_j^T \cdot {}^{L_j}F_r\right] \cdot (\dot{q}_{jr} - \dot{q}_j) \\ \kappa_j^\zeta = \begin{cases} 0 & \hat{\zeta}_j \le 1/k_j^+ \quad \text{and} \quad s_j^\zeta \le 0 \\ 0 & \hat{\zeta}_j \ge 1/k_j^- \quad \text{and} \quad s_j^\zeta \ge 0 \\ 1 & \text{otherwise} \end{cases} \end{gathered} \tag{31}$$

where $\rho_{j\gamma} > 0$ and $\rho_j^\zeta > 0$ denote the update gains. The terms $(Y_{jr})_\gamma$ and $(\theta_j)_\gamma$ denote the γth elements of Y_{jr} and θ_j, respectively, and $(\cdot)^+$ and $(\cdot)^-$ denote the known upper and lower bounds of $(\cdot)$.

Combining Eqs. (28) and (29) gives

$$\begin{aligned} I_j^* \cdot (\ddot{q}_{jr} - \ddot{q}_j) &= -Z_j^T \cdot \left({}^{L_j}F_r - {}^{L_j}F\right) + k_j \cdot (I_{cjd} - I_{cj}) \\ &- \left(d_j + k_{vj}^* \cdot k_j\right) \cdot (\dot{q}_{jr} - \dot{q}_j) - \sigma_j \cdot k_{pj}^* \cdot k_j \cdot (q_{jd} - q_j) \\ &+ Y_{jr} \cdot (\theta_j - \hat{\theta}_j) + \left[Y_{jr} \cdot \hat{\theta}_j + Z_j^T \cdot {}^{L_j}F_r\right] \cdot k_j \cdot (\zeta_j - \hat{\zeta}_j) \end{aligned} \tag{32}$$

The corresponding nonnegative accompanying function is defined as

$$\begin{aligned} V_j^c &= \tfrac{1}{2} \cdot I_j^* \cdot (\dot{q}_{jr} - \dot{q}_j)^2 + \sigma_j \cdot \tfrac{1}{2} \cdot k_{pj}^* \cdot k_j \cdot (q_{jd} - q_j)^2 \\ &+ \tfrac{1}{2} \cdot (\theta_j - \hat{\theta}_j)^T \cdot \Gamma_j \cdot (\theta_j - \hat{\theta}_j) + \tfrac{1}{2} \cdot k_j \cdot (\zeta_j - \hat{\zeta}_j)^2 / \rho_j^\zeta \end{aligned} \tag{33}$$

where $\Gamma_j = \text{diag}\{1/\rho_{j1}, 1/\rho_{j2}\}$. In view of Eqs. (32), (8), (30), and (31), the time derivative of Eq. (33) is derived as

$$\begin{aligned} \dot{V}_j^c &= -\left(d_j + k_{vj}^* \cdot k_j\right) \cdot (\dot{q}_{jr} - \dot{q}_j)^2 \\ &- \sigma_j \cdot [(\dot{q}_{jr} - \dot{q}_j) - (\dot{q}_{jd} - \dot{q}_j)] \cdot k_{pj}^* \cdot k_j \cdot (q_{jd} - q_j) \\ &+ (\theta_j - \hat{\theta}_j)^T \cdot \left[Y_{jr}^T \cdot (\dot{q}_{jr} - \dot{q}_j) - \Gamma_j \cdot \dot{\hat{\theta}}_j\right] + k_j \cdot (\zeta_j - \hat{\zeta}_j) \\ &\times \left[\left(Y_{jr} \cdot \hat{\theta}_j + Z_j^T \cdot {}^{L_j}F_r\right) \cdot (\dot{q}_{jr} - \dot{q}_j) - \dot{\hat{\zeta}}_j \big/ \rho_j^\zeta\right] \\ &- (\dot{q}_{jr} - \dot{q}_j) \cdot Z_j^T \cdot \left({}^{L_j}F_r - {}^{L_j}F\right) \\ &+ k_j \cdot (I_{cjd} - I_{cj}) \cdot (\dot{q}_{jr} - \dot{q}_j) \\ &\le -\left(d_j + k_{vj}^* \cdot k_j\right) \cdot (\dot{q}_{jr} - \dot{q}_j)^2 \\ &- \sigma_j \cdot \lambda \cdot k_{pj}^* \cdot k_j \cdot (q_{jd} - q_j)^2 \\ &+ W_{T_j} - W_{L_j} + k_j \cdot (I_{cjd} - I_{cj}) \cdot (\dot{q}_{jr} - \dot{q}_j) \end{aligned} \tag{34}$$

because from Eqs. (30), (31), and (4), it gives

$$\begin{aligned} &(\theta_j - \hat{\theta}_j)^T \cdot \left[Y_{jr}^T \cdot (\dot{q}_{jr} - \dot{q}_j) - \Gamma_j \cdot \dot{\hat{\theta}}_j\right] \\ &= \sum_{\gamma=1}^{2} \left[(\theta_j)_\gamma - (\hat{\theta}_j)_\gamma\right] \cdot s_{j\gamma} \cdot (1 - \kappa_{j\gamma}) \le 0 \end{aligned} \tag{35}$$

$$\begin{aligned} &k_j \cdot (\zeta_j - \hat{\zeta}_j) \cdot \left[\left(Y_{jr} \cdot \hat{\theta}_j + Z_j^T \cdot {}^{L_j}F_r\right) \cdot (\dot{q}_{jr} - \dot{q}_j) - \dot{\hat{\zeta}}_j \big/ \rho_j^\zeta\right] \\ &= k_j \cdot (\zeta_j - \hat{\zeta}_j) \cdot s_j^\zeta \cdot \left(1 - \kappa_j^\zeta\right) \le 0 \end{aligned} \tag{36}$$

$$\begin{aligned} &-(\dot{q}_{jr} - \dot{q}_j) \cdot Z_j^T \cdot \left({}^{L_j}F_r - {}^{L_j}F\right) \\ &= -\left({}^{L_j}X_r - {}^{L_j}X\right)^T \cdot \left({}^{L_j}F_r - {}^{L_j}F\right) \\ &+ \left[{}^{T_j}U_{L_j}^T \cdot \left({}^{T_j}X_r - {}^{T_j}X\right)\right]^T \cdot \left({}^{L_j}F_r - {}^{L_j}F\right) = -W_{L_j} + W_{T_j} \end{aligned} \tag{37}$$

Equation (34) indicates that, when the motor current servo loop has an ideal transfer function of 1, i.e., $I_{cjd} = I_{cj}$, the dynamic interactions between the jth joint and its connected links are completely represented by $W_{T_j} - W_{L_j}$, the VPFs at the two cutting points of the joint. The term $W_{T_j} - W_{L_j}$ will be treated in Sec. VI.

Note that, if k_j is known, by setting $\hat{\zeta}_j = \zeta_j = 1/k_j$, the motor current control changes to conventional motor torque control and Eq. (31) is omitted.

Motor Voltage Control

Motor voltage control can be used to replace motor current control when $I_{cjd} \ne I_{cj}$.

The motor dynamics of the jth joint can be written as

$$a_j \cdot \dot{I}_{cj} + b_j \cdot I_{cj} + c_j \cdot \dot{q}_j = u_j \tag{38}$$

where u_j denotes the control voltage. The term I_{cj} denotes the motor armature current, a_j represents the inductance of the motor, b_j denotes the armature resistance, and c_j denotes the motor electromotive force constant.

The control u_j is designed as

$$u_j = D_j \cdot \mathrm{sign}(I_{cjd} - I_{cj}) + Y_j^m \cdot \hat{\theta}_j^m + k_{\tau j} \cdot (I_{cjd} - I_{cj}) \quad (39)$$

where $Y_j^m = [I_{cj} \quad \dot{q}_j \quad \dot{q}_{jr} - \dot{q}_j]$, $\theta_j^m = [b_j \quad c_j \quad k_j]^T$, and $k_{\tau j} > 0$. The term I_{cjd} is designed in Eq. (29), whereas I_{cj} is a measured motor armature current. The term D_j in Eq. (39) has to satisfy

$$D_j \geq |a_j \cdot \dot{I}_{cjd}| \quad (40)$$

The term $\hat{\theta}_j^m$ is updated through

$$\left(\dot{\hat{\theta}}_j^m\right)_\gamma = \rho_{j\gamma}^m \cdot \kappa_{j\gamma}^m \cdot s_{j\gamma}^m; \qquad \gamma = 1, 2, 3$$

$$s_{j\gamma}^m = \left(Y_j^m\right)_\gamma^T \cdot (I_{cjd} - I_{cj}) \quad (41)$$

$$\kappa_{j\gamma}^m = \begin{cases} 0 & \left(\hat{\theta}_j^m\right)_\gamma \leq \left(\theta_j^m\right)_\gamma^- \quad \text{and} \quad s_{j\gamma}^m \leq 0 \\ 0 & \left(\hat{\theta}_j^m\right)_\gamma \geq \left(\theta_j^m\right)_\gamma^+ \quad \text{and} \quad s_{j\gamma}^m \geq 0 \\ 1 & \text{otherwise} \end{cases}$$

where $\rho_{j\gamma}^m > 0$ denotes the update gain for the γth parameter. The terms $(Y_j^m)_\gamma$ and $(\theta_j^m)_\gamma$ denote the γth elements of Y_j^m and θ_j^m, respectively, and $(\theta_j^m)_\gamma^+$ and $(\theta_j^m)_\gamma^-$ denote the known upper and lower bounds of the physical parameter $(\theta_j^m)_\gamma$.

The corresponding nonnegative accompanying function is defined as

$$V_j^v = V_j^c + \tfrac{1}{2} \cdot a_j \cdot (I_{cjd} - I_{cj})^2 + \tfrac{1}{2} \cdot \left(\theta_j^m - \hat{\theta}_j^m\right)^T \cdot \Gamma_j^m \cdot \left(\theta_j^m - \hat{\theta}_j^m\right) \quad (42)$$

where V_j^c is defined in Eq. (33) and $\Gamma_j^m = \mathrm{diag}\{1/\rho_{j1}^m, 1/\rho_{j2}^m, 1/\rho_{j3}^m, \}$. Substituting Eq. (39) into Eq. (38) gives

$$a_j \cdot (\dot{I}_{cjd} - \dot{I}_{cj}) = [a_j \cdot \dot{I}_{cjd} - D_j \cdot \mathrm{sign}(I_{cjd} - I_{cj})] + Y_j^m \cdot \left(\theta_j^m - \hat{\theta}_j^m\right) - k_{\tau j} \cdot (I_{cjd} - I_{cj}) - k_j \cdot (\dot{q}_{jr} - \dot{q}_j) \quad (43)$$

In view of Eqs. (34), (40), (41), and (43), the time derivative of Eq. (42) can be obtained as

$$\dot{V}_j^v \leq -\left(d_j + k_{vj}^* \cdot k_j\right) \cdot (\dot{q}_{jr} - \dot{q}_j)^2 - \sigma_j \cdot \lambda \cdot k_{pj}^* \cdot k_j \times (q_{jd} - q_j)^2 - k_{\tau j} \cdot (I_{cjd} - I_{cj})^2 + W_{T_j} - W_{L_j} \quad (44)$$

because from Eq. (41)

$$\left(\theta_j^m - \hat{\theta}_j^m\right)^T \cdot \left[Y_j^{mT} \cdot (I_{cjd} - I_{cj}) - \Gamma_j^m \cdot \dot{\hat{\theta}}_j^m\right] = \sum_{\gamma=1}^{3} \left[\left(\theta_j^m\right)_\gamma - \left(\hat{\theta}_j^m\right)_\gamma\right] \cdot s_{j\gamma}^m \cdot \left(1 - \kappa_{j\gamma}^m\right) \leq 0 \quad (45)$$

In the motor voltage control mode, Eq. (40) is a sufficient condition that ensures Eq. (44). In view of Eq. (29), $\dot{I}_{cjd}$ is a linear function of $(\mathrm{d}/\mathrm{d}t)({}^{L_j}F_r)$ and $\ddot{q}_j$. Using Eqs. (21), (22), (14), and (12), $(\mathrm{d}/\mathrm{d}t)({}^{L_j}F_r)$ can be represented by a linear function of $[\ddot{q}^T \; (\mathrm{d}/\mathrm{d}t)({}^BX)^T]^T$. Therefore, $\dot{I}_{cjd}$ is a linear function of $[\ddot{q}^T \; (\mathrm{d}/\mathrm{d}t)({}^BX)^T]^T$, which contains both joint and base accelerations and is bounded by the joint drive torques $\tau = [k_1 \cdot I_{c1}, \ldots, k_j \cdot I_{cj}, \ldots, k_9 \cdot I_{c9}]^T$. Thus, we can specify

$$D_j = a_{\tau j}(t) \cdot \|I_c\| + b_{\tau j}(t) \quad (46)$$

so as to hold Eq. (40), where $a_{\tau j}(t)$ and $b_{\tau j}(t)$ are two bounded positive scalars that are functions of measurable variables.

This subsection provides a flexible way for performing adaptive control of each joint. Motor torque control can be used only when $I_{cjd} = I_{cj}$, i.e., the current servo loop has an ideal transfer function of 1. Otherwise, motor voltage control is recommended.

On the basis of motor current control, which gives I_{cjd} from Eq. (29), motor voltage control is designed by incorporating the motor dynamics. Therefore, some terms related to the motor dynamics are added to the right-hand sides of both Eq. (42) and Eq. (44). However, an important point is that both motor voltage control and motor current control impose the same dynamic interactions $(W_{T_j} - W_{L_j})$ on the connected links; see Eqs. (44) and (34) with $I_{cjd} = I_{cj}$. This indicates that the dynamic interactions between the jth joint and its connected links are completely represented by the VPFs at the two cutting points of the joint, which are invariant to the control mode used. Therefore, motor voltage control and motor current control can be used alternatively and can be replaced with each other.

Similar as for rigid links, every joint parameter can be updated within its upper and lower bounds independently; see Eqs. (30), (31), and (41).

VI. Lyapunov Stability

The stability analysis consists of two steps. In the first step, each subsystem (link or joint) is assigned a corresponding nonnegative accompanying function as described in the preceding section. Then, in the second step, the system Lyapunov function is formed by merely adding all nonnegative accompanying functions assigned for the subsystems, i.e.,

$$V = V_B + \sum_{j=1}^{9} \left(V_{L_j} + V_j\right) \quad (47)$$

where

$$V_j = \begin{cases} V_j^c & \text{motor current control} \\ V_j^v & \text{motor voltage control} \end{cases}$$

In view of Eqs. (17), (24–26), (34) with $I_{cjd} = I_{cj}$, and (44), all VPFs at the cutting points of the subsystems cancel out in $\dot{V}$, i.e.,

$$-W_{T_1} - \sum_{j=7}^{9} W_{T_j} + \sum_{j=1}^{5} \left(W_{L_j} - W_{T_{(j+1)}}\right) + \sum_{j=6}^{9} W_{L_j} + \sum_{j=1}^{9} \left(W_{T_j} - W_{L_j}\right) = 0$$

It follows that

$$\dot{V} \leq -\sum_{\alpha} \left[\left({}^\alpha X_r - {}^\alpha X\right)^T \cdot K_\alpha \cdot \left({}^\alpha X_r - {}^\alpha X\right) + \Upsilon_\alpha\right] - \sum_{j=1}^{9} \left[\left(d_j + k_{vj}^* \cdot k_j\right) \cdot (\dot{q}_{jr} - \dot{q}_j)^2 + \sigma_j \cdot \lambda \cdot k_{pj}^* \cdot k_j \cdot (q_{jd} - q_j)^2 + \delta_j \cdot k_{\tau j} \cdot (I_{cjd} - I_{cj})^2\right] \leq 0 \quad (48)$$

where Υ_α is defined in Eq. (17) and

$$\delta_j = \begin{cases} 0 & \text{motor current control} \\ 1 & \text{motor voltage control} \end{cases}$$

The Lyapunov stability is therefore guaranteed. The term $\dot{V} \leq 0$ implies that V is a nonincreasing positive function. Thus, it follows from Eqs. (17) and (48) that

$$\dot{V} \leq -\lambda \cdot k_B \cdot {}^B\mu^T \cdot {}^B\mu$$

such that

$$\int_0^\infty \left(\lambda \cdot k_B \cdot {}^B\mu^T \cdot {}^B\mu\right) \mathrm{d}t \leq -\int_0^\infty \dot{V} \, \mathrm{d}t \leq V(0) < +\infty$$

i.e., ${}^B\mu \in L_2$. Note that ${}^Ee$, ${}^E\mu$, $q_{md} - q_m$, $\dot{q}_r - \dot{q}$, ${}^BX_r - {}^BX$, and $I_{cjd} - I_{cj}$ can be handled in the same way. It follows from Eqs. (16), (33), (42), (47), and (48) that

$$ {}^B\mu \in L_2 \bigcap L_\infty $$

$$ [{}^Ee^T, {}^E\mu^T]^T \in L_2 \bigcap L_\infty \qquad \sigma = 0 $$

$$ q_{md} - q_m \in L_2 \bigcap L_\infty \qquad \sigma = 1 $$

$$ \dot{q}_r - \dot{q} \in L_2 \bigcap L_\infty $$

$$ {}^BX_r - {}^BX \in L_2 \bigcap L_\infty $$

$$ I_{cjd} - I_{cj} \in L_2 \bigcap L_\infty \qquad \text{motor voltage control} $$

The stability results ensure $[\dot{q}_{wr}^T \;\; {}^B\nu_r^T]^T - [\dot{q}_w^T \;\; {}^B\nu^T]^T \to 0$. The nonholonomic constraints imply that $[\dot{q}_w^T \;\; {}^B\nu^T]^T$ is a function of $[\dot{q}_m^T \;\; {}^B\omega^T]^T$ (Ref. 7). Therefore, the boundedness of $[\dot{q}_{wr}^T \;\; {}^B\nu_r^T]^T$ is guaranteed.

their corresponding required velocities. Using Eq. (12), the required extended accelerations are linear functions of $[\ddot{q}_{wr}^T \;\; (\mathrm{d}/\mathrm{d}t)({}^B\nu_r)^T]^T$, i.e., $(\mathrm{d}/\mathrm{d}t)({}^\alpha X_r) = A_{x\alpha} \cdot [\ddot{q}_{wr}^T \;\; (\mathrm{d}/\mathrm{d}t)({}^B\nu_r)^T]^T + B_{x\alpha}$, where $A_{x\alpha}$ and $B_{x\alpha}$ are a known matrix and a known vector, respectively. Therefore, $(\mathrm{d}/\mathrm{d}t)({}^\alpha X_r)$ is represented as a pair $(A_{x\alpha}, B_{x\alpha})$. Obviously, $[\dot{q}_{wr}^T \;\; {}^B\nu_r^T]^T$ can be obtained through integrating $[\ddot{q}_{wr}^T \;\; (\mathrm{d}/\mathrm{d}t)({}^B\nu_r)^T]^T$.

In part 2, Eqs. (14) and (15) yield the required net force/moments of all rigid bodies and the corresponding parameter adaptation. Note that all required net force/moments are linear functions of $[\ddot{q}_{wr}^T \;\; (\mathrm{d}/\mathrm{d}t)({}^B\nu_r)^T]^T$.

In part 3, the constraint equation (23) is considered. Based on the calculations carried out in part 2, Eq. (23) can be written as

$$ \mathcal{A}_f \cdot \begin{bmatrix} \ddot{q}_{wr} \\ \dfrac{\mathrm{d}}{\mathrm{d}t}\left({}^B\nu_r\right) \end{bmatrix} + \mathcal{B}_f = 0 \qquad (49) $$

where

$$ \mathcal{A}_f = \begin{cases} \left[0_{6\times 9}, \hat{M}_B, {}^BU_{L_1}\cdot\hat{M}_{L_1}, \ldots, {}^BU_{L_j}\cdot\hat{M}_{L_j}, \ldots, {}^BU_{L_9}\cdot\hat{M}_{L_9}\right]\mathcal{T}\cdot\begin{bmatrix} 0_{6\times 6} \\ I_6 \\ 0_{3\times 6}\end{bmatrix} & \sigma = 1 \\ \left[0_{6\times 9}, \hat{M}_B, {}^BU_{L_1}\cdot\hat{M}_{L_1}, \ldots, {}^BU_{L_j}\cdot\hat{M}_{L_j}, \ldots, {}^BU_{L_9}\cdot\hat{M}_{L_9}\right]\mathcal{T}\cdot & \\ \begin{bmatrix} J^{-1}\cdot {}^EU_{L_6}^T & 0 & -J^{-1}\cdot {}^BU_{L_6}^T \\ 0 & I_3 & 0 \\ 0 & 0 & I_6 \end{bmatrix}\cdot\begin{bmatrix} 0_{6\times 6} \\ I_6 \\ 0_{3\times 6}\end{bmatrix} & \sigma = 0 \end{cases} $$

is a 6×6 known matrix and $\mathcal{B}_f \in R^6$ is a known vector. The term $\hat{M}_\alpha$, $\alpha \in \{B, L_1, \ldots, L_j, \ldots, L_9\}$, denotes the estimate of M_α defined in Eq. (13). For exact inertial parameters, the invertibility of $\mathcal{A}_f$ is guaranteed by proper arrangement of the three reaction wheels. Therefore, it is believed that, with an appropriate choice of the upper and lower bounds of these inertial parameters, the invertibility of $\mathcal{A}_f$ still holds. Equation (49) gives the solution of $[\ddot{q}_{wr}^T \;\; (\mathrm{d}/\mathrm{d}t)({}^B\nu_r)^T]^T$. After that, ${}^{L_j}F_r$, $j = 1, 2, \ldots, 9$, is calculated through Eqs. (21) and (22).

In part 4, either Eqs. (29–31) in the case of motor current control or Eqs. (29–31) together with Eqs. (39–41) in the case of motor

VII. Control Algorithm Overview

The control system, illustrated in Fig. 2, consists of four parts. Parts 2 and 4 can be carried out in parallel for all subsystems. Only parts 1 and 3 should take into account the overall design.

In part 1, the joint positions/velocities of the manipulator, the orientation of the base, the linear/angular velocity of the base, and the velocities of the reaction wheels are measured. Equation (5) is calculated to get the extended velocities. Then control specification is conducted in terms of either Eq. (8) (joint space) or Eq. (10) (Cartesian space). The required extended velocities are calculated from Eq. (11) and Eq. (6) or (7) by replacing the real velocities by

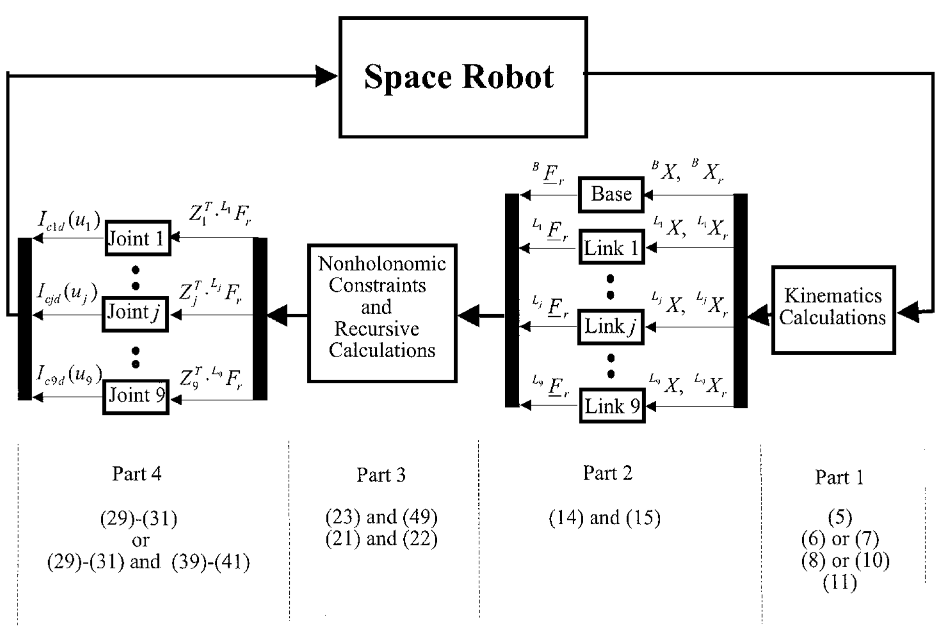

Fig. 2 Control algorithm.

voltage control are used for each joint. Equation (46) is used to ensure Eq. (40).

Most of the computations are performed in parts 2 and 4 in which parallel processing is possible. The information exchange between these parts is quite limited. Meanwhile, each parameter can be adjusted independently within its upper and lower bounds without coupling to other parameters [see Eqs. (15), (30), (31), and (41)]. This makes decentralized parameter adaptation possible. All these features imply the possibility of a modularity-based adaptive control design that can be implemented in modular hardware particularly designed for rigid bodies and joints to meet the practical case of spaceborne computers with relatively low processing capability.[11]

VIII. Free-Floating Single-Arm Space Robots

Free floating means that the three reaction wheels are not controlled with zero torque, i.e., $I_{cj} = 0$ for $j = 7, 8, 9$. Accordingly, from Eq. (29) it follows that

$$Y_{jr} \cdot \hat{\theta}_j + Z_j^T \cdot {}^{Lj}F_r + \hat{k}_j \cdot k_{vj}^* \cdot (\dot{q}_{jr} - \dot{q}_j) = 0 \qquad j = 7, 8, 9 \quad (50)$$

where $\hat{k}_j = 1/\hat{\zeta}_j$. Equation (23) plus Eq. (50) gives a total of nine constraint equations. Therefore, nine instead of six variables should be released to meet these constraints. Consequently, the independent velocity equations (6) and (7) should be changed to

$$\begin{bmatrix} \dot{q} \\ {}^BX \end{bmatrix} = \begin{bmatrix} \dot{q}_m \\ \dot{q}_w \\ {}^BX \end{bmatrix} = \begin{bmatrix} I_6 \\ 0 \end{bmatrix} \cdot \dot{q}_m + \begin{bmatrix} 0 \\ I_9 \end{bmatrix} \cdot \begin{bmatrix} \dot{q}_w \\ {}^BX \end{bmatrix} \quad (51)$$

for the joint space specification ($\sigma = 1$) or

$$\begin{bmatrix} \dot{q} \\ {}^BX \end{bmatrix} = \begin{bmatrix} J^{-1} \cdot {}^EU_{L_6}^T & 0 & -J^{-1} \cdot {}^BU_{L_6}^T \\ 0 & I_3 & 0 \\ 0 & 0 & I_6 \end{bmatrix} \times \left(\begin{bmatrix} I_6 \\ 0 \end{bmatrix} \cdot {}^EX + \begin{bmatrix} 0 \\ I_9 \end{bmatrix} \cdot \begin{bmatrix} \dot{q}_w \\ {}^BX \end{bmatrix} \right) \quad (52)$$

for the Cartesian space specification ($\sigma = 0$). Only $\dot{q}_m$ or ${}^EX$ is subject to the control specifications as

$$\dot{q}_{mr} = \dot{q}_{md} + \lambda \cdot (q_{md} - q_m) \quad (53)$$

or

$${}^EX_r = \mathrm{diag}\{{}^ER_I, {}^ER_I\} \cdot \begin{bmatrix} \nu_{E_d} \\ \omega_{E_d} \end{bmatrix} + \lambda \cdot \begin{bmatrix} {}^Ee \\ {}^E\mu \end{bmatrix} \quad (54)$$

whereas $[\dot{q}_w^T \;\; {}^BX^T]^T \in R^9$ is released to meet the nine constraint equations of Eqs. (23) and (50).

Combining Eq. (23) with Eq. (50) yields

$$\mathcal{A}_{ff} \cdot \begin{bmatrix} \ddot{q}_{wr} \\ \dfrac{\mathrm{d}}{\mathrm{d}t}\left({}^BX_r\right) \end{bmatrix} + \mathcal{B}_{ff} = 0 \quad (55)$$

where

$$\mathcal{A}_{ff} = \begin{cases} \Pi_f \cdot \mathcal{T} \cdot \begin{bmatrix} 0_{6\times 6} \\ I_9 \end{bmatrix} & \sigma = 1 \\ \Pi_f \cdot \mathcal{T} \cdot \begin{bmatrix} J^{-1} \cdot {}^EU_{L_6}^T & 0 & -J^{-1} \cdot {}^BU_{L_6}^T \\ 0 & I_3 & 0 \\ 0 & 0 & I_6 \end{bmatrix} \cdot \begin{bmatrix} 0_{6\times 6} \\ I_9 \end{bmatrix} & \sigma = 0 \end{cases}$$

$$\Pi_f = \begin{bmatrix} 0_{6\times 6} & \multicolumn{3}{c}{0_{6\times 3}} & \hat{M}_B & {}^BU_{L_1} \cdot \hat{M}_{L_1} & \ldots & {}^BU_{L_7} \cdot \hat{M}_{L_7} & {}^BU_{L_8} \cdot \hat{M}_{L_8} & {}^BU_{L_9} \cdot \hat{M}_{L_9} \\ & \hat{I}_7^* & 0 & 0 & & & & Z_7^T \cdot \hat{M}_{L_7} & 0_{1\times 6} & 0_{1\times 6} \\ 0_{3\times 6} & 0 & \hat{I}_8^* & 0 & 0_{3\times 6} & 0_{3\times 6} & \ldots & 0_{1\times 6} & Z_8^T \cdot \hat{M}_{L_8} & 0_{1\times 6} \\ & 0 & 0 & \hat{I}_9^* & & & & 0_{1\times 6} & 0_{1\times 6} & Z_9^T \cdot \hat{M}_{L_9} \end{bmatrix}$$

The term $\mathcal{A}_{ff} \in R^{9\times 9}$ is a known matrix, and $\mathcal{B}_{ff} \in R^9$ is a known vector. The invertibility of $\mathcal{A}_{ff}$ is guaranteed in the same way as $\mathcal{A}_f$ in the last section. Equation (55) gives the solution for $[\ddot{q}_{wr}^T \;\; (\mathrm{d}/\mathrm{d}t)({}^BX_r)^T]^T$. After that $[\dot{q}_{wr}^T \;\; {}^BX_r^T]^T$ is obtained through integrating $[\ddot{q}_{wr}^T \;\; (\mathrm{d}/\mathrm{d}t)({}^BX_r)^T]^T$.

With the same Lyapunov function defined in Eq. (47), by replacing Eq. (49) with Eq. (55) the Lyapunov stability is still guaranteed with all signals bounded.

IX. Potential Extensions

The proposed approach can be extended easily to treat more complicated cases due to its modular structure in both control design and stability analysis.

For systems of h six-joint manipulators mounted on a common base, the approach can be applied directly. Each arm is treated independently. The difference is only related to the base. Consequently, Eq. (23) should be changed to

$${}^B\underline{F}_r + \sum_{i=1}^{h}\sum_{j=1}^{6} {}^BU_{L_{ij}} \cdot {}^{L_{ij}}\underline{F}_r + \sum_{j=7}^{9} {}^BU_{L_j} \cdot {}^{L_j}\underline{F}_r = 0$$

The Lyapunov function (47) is also changed to

$$V = V_B + \sum_{i=1}^{h}\sum_{j=1}^{6}\left(V_{L_{ij}} + V_{ij}\right) + \sum_{j=7}^{9}\left(V_{L_j} + V_j\right)$$

When the h manipulators grasp a rigid object, closed kinematic loops are formed, and the corresponding internal forces are generated. However, note that these internal forces just exist within the closed kinematic loops without making any contribution to the base. Thus, the internal force control problem can be isolated.

Two space robots grasping an object (see Ref. 17) have $15 + 15 - 6 = 24$ DOF. This system can be viewed as a special tree type 15-joint redundant manipulator mounted on a base. Suppose the base of the first space robot is viewed as the base, while the first manipulator and the second space robot form the redundant manipulator of which the 6th link represents the 6th links of the two space robots plus the payload, and the 12th link represents the base of the second space. Thus, the proposed approach can be applied directly. Certainly, optimization can be performed with respect to the redundant manipulator.

X. Computer Simulations

The simulated system is a one-arm space robot moving in a plane. The manipulator has three rotational joints. Only one reaction wheel is considered. Therefore, there are total seven motion DOF.

Two typical cases are simulated. Case 1 is for robot joint tracking control with base orientation control (free flying). The total control dimension is four, whereas the released dimension is three (for the nonholonomic constraints). Case 2 is for robot joint tracking control without base orientation control (free floating). The total control dimension is three, and the released dimension is therefore four.

The control objective of case 1 is to make the three joints of the manipulator and the orientation of the base track their desired trajectories while starting from considerable initial errors. The desired trajectories are designed as

$$[1.2 - \text{plan} \quad 1.3 + \text{plan} \quad 1.3 + \text{plan} \quad 0]$$

where

$$\text{plan} = \begin{cases} 0.2 \cdot \cos[(\pi/20) \cdot t] & 0 \le t \le 20 \\ -0.2 & t > 20 \end{cases}$$

with initial positions

$$[1.1 \quad 1.4 \quad 1.55 \quad -0.05]^T \in R^4$$

In the planar case, there are four parameters

$$\theta_\alpha = \left\{(m) \quad (m \cdot r_{x\alpha}) \quad (m \cdot r_{y\alpha}) \quad \left[I_\alpha + m \cdot \left(r_{x\alpha}^2 + r_{y\alpha}^2\right)\right]\right\}^T \qquad \alpha \in \{B, L_1, \ldots, L_4\}$$

for the base or each link, where m is the mass. The terms $r_{x\alpha}$ and $r_{y\alpha}$ denote the coordinates of the mass center expressed in frame α.

The parameters used in the simulations are listed in Tables 1 and 2. All motors are working with motor voltage control mode. The upper and lower bounds of each parameter are set to be 200 and 50%, respectively, of the real value. All parameters are updated starting from their lower bounds.

The sampling time in the simulations is chosen as 5 ms. However, 1 ms is used for calculating Eqs. (38) and (39) in the motor voltage control mode.

Table 1 Parameters of the rigid bodies

Area	l, m	r_x, m	r_y, m	m, kg	I, kg · m^2
Base		0.1	0.1	5000	1000
Link 1	5.0	2.5	0.0	100	100
Link 2	5.0	2.5	0.0	100	100
Link 3	2.0	1.5	0.0	1000	100
Reaction wheel	——	0.0	0.0	100	50

Table 2 Parameters of the joints

Joint	I^*, kg · m^2	d, N · m · s	k, N · m/A	a, H	b, Ω	c, V · s
1	100	5.0	200	0.005	5.0	20
2	100	5.0	200	0.005	5.0	20
3	100	5.0	200	0.005	5.0	20
4	5	2.0	20	0.010	5.0	4

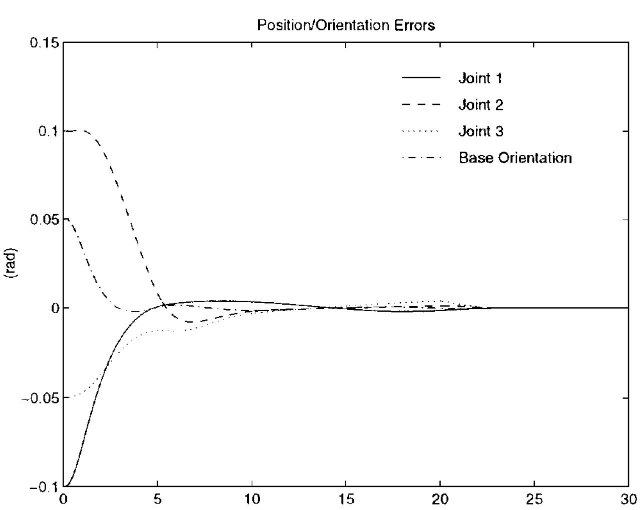

Fig. 3 Position/orientation errors in free flying.

The control constants and gains are

$$\lambda = 1.0, \qquad k_B = 50$$

$$K_B = \begin{bmatrix} 2500 & & \\ & 2500 & \\ & & 1000 \end{bmatrix}$$

$$K_{L_1} = K_{L_2} = \begin{bmatrix} 500 & & \\ & 500 & \\ & & 1000 \end{bmatrix}$$

$$K_{L_3} = \begin{bmatrix} 1000 & & \\ & 1000 & \\ & & 2000 \end{bmatrix}; \qquad K_{L_4} = \begin{bmatrix} 50 & & \\ & 50 & \\ & & 50 \end{bmatrix}$$

$$k_{v1}^* = k_{v2}^* = k_{v3}^* = 2.5, \qquad k_{v4}^* = 10$$

$$k_{p1}^* = k_{p2}^* = k_{p3}^* = 0.25$$

$$k_{\tau 1} = k_{\tau 2} = k_{\tau 3} = 2.0, \qquad k_{\tau 4} = 5.0$$

The simulation results are illustrated in Figs. 3–5. Figure 3 gives position/orientation tracking results in free flying. The control voltages of all motors are presented in Fig. 4. Figure 5 gives position/orientation tracking results in free floating. These figures

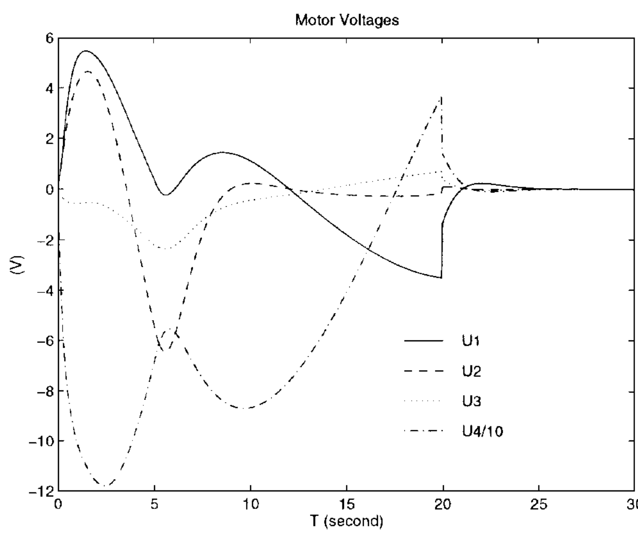

Fig. 4 Control voltages in free flying.

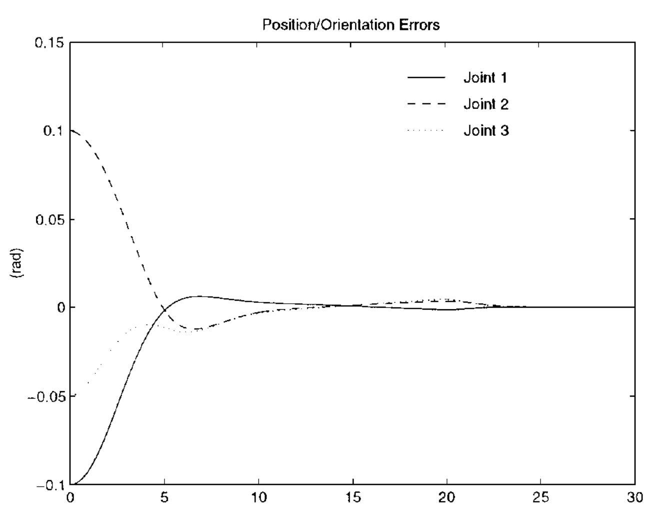

Fig. 5 Position/orientation errors in free floating.

demonstrate good tracking performance with reasonably bounded control input.

XI. Conclusion

A general modularity-based approach named virtual decomposition is proposed for adaptive control of space robots. Virtual decomposition results in a modular structure for both control design and stability analysis.

For control design, the control design of the complete system is converted into the control design of each subsystem (rigid body or joint), whereas the nonholonomic constraints are represented by a set of constraint equations about the required accelerations. Only the dynamics of the rigid body and the dynamics of the joint incorporating motor are needed in the control design of the subsystems. Parameter adaptation is carried out independently for each parameter. Most of the computations in the control algorithm can be performed in parallel. All of these features support the possibility of implementing the control algorithm in modular hardware particularly designed for rigid bodies and joints to meet the practical case of spaceborne computers with relatively low processing capability.

For stability analysis, a modularity-based two-step approach is presented. The first step searches for a nonnegative accompanying function for each subsystem (rigid link and joint). This step is relatively simple because of the simple dynamics of the subsystems. The second step is to form the system Lyapunov function. It is also simple because the system Lyapunov function is formed by merely adding all nonnegative accompanying functions assigned to the subsystems.

Computer simulations have been conducted to verify the validity of the approach. The simulation results support the theoretical results.

The proposed approach can be extended to deal with more complicated space robotic systems, including multiple robot arms mounted on a common base, coordinated multiple robot arms mounted on a common base, and coordinated multiple space robots.

Appendix: Proof of Equation (17)

Subtracting Eq. (13) from Eq. (14) gives

$$
\begin{aligned}
{}^{\alpha}\underline{F}_r - {}^{\alpha}\underline{F} &= M_\alpha\left[\frac{\mathrm{d}}{\mathrm{d}t}\left({}^{\alpha}X_r\right) - \frac{\mathrm{d}}{\mathrm{d}t}\left({}^{\alpha}X\right)\right] + C_\alpha({}^{\alpha}\omega)\cdot\left({}^{\alpha}X_r - {}^{\alpha}X\right)\\
&+ K_\alpha\cdot\left({}^{\alpha}X_r - {}^{\alpha}X\right) + P_\alpha - Y_{\alpha r}\cdot(\theta_\alpha - \hat{\theta}_\alpha) \qquad \text{(A1)}
\end{aligned}
$$

Note that M_α is a constant matrix and $C_\alpha({}^{\alpha}\omega)$ is a skew-symmetric matrix. Differentiating Eq. (16) and then using Eq. (A1) gives

$$
\begin{aligned}
\dot{V}_\alpha &= \left({}^{\alpha}X_r - {}^{\alpha}X\right)^T\cdot M_\alpha\left[\frac{\mathrm{d}}{\mathrm{d}t}\left({}^{\alpha}X_r\right) - \frac{\mathrm{d}}{\mathrm{d}t}\left({}^{\alpha}X\right)\right]\\
&- (\theta_\alpha - \hat{\theta}_\alpha)^T\cdot\Gamma_\alpha\cdot\dot{\hat{\theta}}_\alpha + \dot{\Psi}_\alpha\\
&= -\left({}^{\alpha}X_r - {}^{\alpha}X\right)^T\cdot K_\alpha\cdot\left({}^{\alpha}X_r - {}^{\alpha}X\right)\\
&- \left[\left({}^{\alpha}X_r - {}^{\alpha}X\right)^T\cdot P_\alpha - \dot{\Psi}_\alpha\right]\\
&+ (\theta_\alpha - \hat{\theta}_\alpha)^T\cdot\left[Y_{\alpha r}^T\cdot\left({}^{\alpha}X_r - {}^{\alpha}X\right) - \Gamma_\alpha\cdot\dot{\hat{\theta}}_\alpha\right]\\
&+ \left({}^{\alpha}X_r - {}^{\alpha}X\right)^T\cdot\left({}^{\alpha}\underline{F}_r - {}^{\alpha}\underline{F}\right) \qquad \text{(A2)}
\end{aligned}
$$

In view of Eqs. (9), (10), and (12), it is easy to obtain

$$
\left({}^{\alpha}X_r - {}^{\alpha}X\right)^T\cdot P_\alpha - \dot{\Psi}_\alpha = \Upsilon_\alpha \qquad \text{(A3)}
$$

where Ψ_α is defined in Eq. (16) and Υ_α is defined in Eq. (17). From Eq. (15) the third term on the right-hand side of Eq. (A2) can be rewritten as

$$
\begin{aligned}
&(\theta_\alpha - \hat{\theta}_\alpha)^T\cdot\left[Y_{\alpha r}^T\cdot\left({}^{\alpha}X_r - {}^{\alpha}X\right) - \Gamma_\alpha\cdot\dot{\hat{\theta}}_\alpha\right]\\
&= \sum_\gamma\left[(\theta_\alpha)_\gamma - (\hat{\theta}_\alpha)_\gamma\right]\cdot s_\gamma^\alpha\cdot\left(1 - \kappa_\gamma^\alpha\right) \le 0 \qquad \text{(A4)}
\end{aligned}
$$

Substituting Eqs. (A3) and (A4) into Eq. (A2) gives Eq. (17).

Acknowledgment

The first author's work was supported by a postdoctoral fellowship awarded by the Katholieke Universiteit Leuven.

References

[1]Xu, Y., and Kanade, T., *Space Robotics: Dynamics and Control*, Kluwer Academic, Boston, MA, 1993.

[2]Ruoff, C. F., and Skaar, S. B., *Teleoperation and Robotics in Space*, Vol. 161, Progress in Astronautics and Aeronautics, AIAA, Washington, DC, 1994.

[3]Longman, R. W., Lindberg, R. E., and Zedd, M. F., "Satellite-Mounted Robot Manipulators—New Kinematics and Reaction Moment Compensation," *International Journal of Robotics Research*, Vol. 6, No. 3, 1987, pp. 87–103.

[4]Dubowsky, S., and Papadopoulos, E., "The Kinematics, Dynamics, and Control of Free-Flying and Free-Floating Space Robotic Systems," *IEEE Transactions on Robotics and Automation*, Vol. RA-9, No. 5, 1993, pp. 531–543.

[5]Egeland, O., and Sagli, J. R., "Coordination of Motion in a Spacecraft/Manipulator System," *International Journal of Robotics Research*, Vol. 12, No. 4, 1993, pp. 366–379.

[6]Spofford, J. R., and Akin, D. L., "Redundancy Control of a Free-Flying Telerobot," *Journal of Guidance, Control, and Dynamics*, Vol. 12, No. 3, 1990, pp. 515–523.

[7]Nakamura, Y., and Mukherjee, R., "Exploiting Nonholonomic Redundancy of Free-Flying Space Robots," *IEEE Transactions on Robotics and Automation*, Vol. RA-9, No. 4, 1993, pp. 499–506.

[8]Papadopoulos, E., and Dubowsky, S., "On the Nature of Control Algorithms for Free-Floating Space Manipulators," *IEEE Transactions on Robotics and Automation*, Vol. 7, No. 6, 1991, pp. 750–758.

[9]Papadopoulos, E., and Dubowsky, S., "Dynamic Singularities in Free-Floating Space Manipulators," *Journal of Dynamic Systems, Measurement, and Control*, Vol. 115, No. 1, 1993, pp. 44–52.

[10]Umetani, Y., and Yoshida, K., "Resolved Motion Rate Control of Space Manipulators with Generalized Jacobian Matrix," *IEEE Transactions on Robotics and Automation*, Vol. RA-5, No. 3, 1989, pp. 303–314.

[11]Oda, M., "Coordinated Control of Spacecraft Attitude and Its Manipulator," Inst. of Electrical and Electronics Engineers International Conf. on Robotics and Automation, Minneapolis, MN, 1996, pp. 732–738.

[12]Jain, A., and Rodriguez, G., "An Analysis of the Kinematics and Dynamics of Underactuated Manipulators," *IEEE Transactions on Robotics and Automation*, Vol. RA-9, No. 5, 1993, pp. 411–422.

[13]Yoshida, K., Kurazume, R., and Umetani, Y., "Dual Arm Coordination in Space Free-Flying Robot," Inst. of Electrical and Electronics Engineers International Conf. on Robotics Automation, Sacramento, CA, 1991, pp. 2516–2521.

[14]Yokokohji, Y., Toyoshima, T., and Yoshikawa, T., "Efficient Computational Algorithm for Trajectory Control of Free-Flying Space Robots with Multiple Arms," *IEEE Transactions on Robotics and Automation*, Vol. RA-9, No. 5, 1993, pp. 571–579.

[15]Murphy, S. H., Wen, J. T., and Saridis, G. N., "Simulation of Cooperating Robot Manipulators on a Mobile Platform," *IEEE Transactions on Robotics and Automation*, Vol. RA-7, No. 4, 1991, pp. 468–477.

[16]Miles, E. S., and Cannon, R. H., Jr., "Utilizing Human Vision and Computer Vision to Direct a Robot in a Semi-Structured via Task-Level Commands," Inst. of Electrical and Electronics Engineers International Conf. on Intelligent Robots and Systems, Vol. 1, Pittsburgh, PA, 1995, pp. 366–371.

[17]Zhu, W. H., Xi, Y. G., and Zhang, Z. J., "Coordinative Control of Two Space Robots Based on Virtual Decomposition," *Proceedings of the Third IEEE Conference on Control Application* (Glasgow, Scotland, UK), Inst. of Electrical and Electronics Engineers, New York, 1994, pp. 327–332.

[18]Dickson, W. C., and Cannon, R. H., Jr., "Experimental Results of Two Free-Flying Robots Capturing and Manipulating a Free-Flying Object," Inst. of Electrical and Electronics Engineers International Conf. on Intelligent Robots and Systems, Vol. 2, Pittsburgh, PA, 1995, pp. 51–58.

[19]Walker, M. W., and Wee, L. B., "Adaptive Control of Space-Based Robot Manipulators," *IEEE Transactions on Robotics and Automation*, Vol. 7, No. 6, 1991, pp. 828–835.

[20]Xu, Y., Shum, H. Y., Lee, J. J., and Kanade, T., "Adaptive Control of Space Robot System with an Attitude Controlled Base," Inst. of Electrical and Electronics Engineers International Conf. on Robotics and Automation, Nice, France, 1992, pp. 2005–2010.

[21]Xu, Y., Shum, H. Y., Kanade, T., and Lee, J. J., "Parameterization and Adaptive Control of Space Robot Systems," *IEEE Transactions on Aerospace and Electronic Systems*, Vol. 30, No. 2, 1994, pp. 435–451.

[22]Gu, Y. L., and Xu, Y., "A Normal Form Augmentation Approach to Adaptive Control of Space Robot Systems," Inst. of Electrical and Electronics Engineers International Conf. on Robotics and Automation, (Atlanta, GA), 1993, pp. 731–737.

[23]Chen, V. W., and Cannon, R. H., Jr., "Experiments in Nonlinear Adaptive Control of Multi-Manipulator Free-Flying Robots," Inst. of Electrical and Electronics Engineers International Conf. on Robotics and Automation, San Diego, CA, 1994, pp. 2213–2220.

[24]Ma, B., and Huo, W., "Adaptive Control of Space Robot System with an Attitude Controlled Base," Inst. of Electrical and Electronics Engineers International Conf. on Robotics and Automation, Nagoya, Japan, 1995, pp. 1265–1270.

[25]Jean, J. H., and Fu, L. C., "On the Adaptive Control of Space Robots," 31st Inst. of Electrical and Electronics Engineers Conf. on Decision and Control, Tucson, AZ, 1992, pp. 1419–1423.

[26]Shin, J. H., Jeong, I. K., Lee, J. J., and Ham, W., "Adaptive Robust Control for Free-Flying Space Robots Using Norm-Bounded Property of Uncertainty," Inst. of Electrical and Electronics Engineers International Conf. on Intelligent Robots and Systems, Pittsburgh, PA, 1995, pp. 59–64.

[27]Wee, L. B., Walker, M. W., and McClamroch, N. H., "An Articulated-Body Model for a Free-Flying Robot and Its Use for Adaptive Motion Control," *IEEE Transactions on Robotics and Automation*, Vol. 13, No. 2, 1997, pp. 264–277.

[28]Tarn, T. J., Bejczy, A. K., Yun, X., and Li, Z., "Effect of Motor Dynamics on Nonlinear Feedback Robot Arm Control," *IEEE Transactions on Robotics and Automation*, Vol. RA-7, No. 1, 1991, pp. 114–122.

[29]Dawson, D. M., Qu, Z., and Carrol, J. J., "Tracking Control of Rigid-Link Electrically-Driven Robot Manipulators," *International Journal of Control*, Vol. 56, No. 5, 1992, pp. 991–1006.

[30]Liu, G., and Goldenberg, A. A., "Robust Control of Robot Manipulators Incorporating Motor Dynamics," *IEEE/IROS'93* (Yokohama, Japan), Inst. of Electrical and Electronics Engineers, New York, 1993, pp. 68–75.

[31]Su, C. Y., and Stepanenko, Y., "Hybrid Adaptive/Robust Motion Control of Rigid-Link Electrically-Driven Robot Manipulators," *IEEE Transactions on Robotics and Automation*, Vol. RA-11, No. 3, 1995, pp. 426–432.

[32]Klumpp, A. R., "Singularity-Free Extraction of a Quaternion from a Direction-Cosine Matrix," *Journal of Spacecraft*, Vol. 13, No. 12, 1976, pp. 754, 755.

[33]Wen, J. T., and Kreutz, K., "The Attitude Control Problems," *IEEE Transactions on Automatic Control*, Vol. AC-36, No. 10, 1991, pp. 1148–1162.

[34]Vafa, Z., and Dubowsky, S., "On the Dynamics of Space Manipulators Using the Virtual Manipulator, with Application to Path Planning," *Journal of the Astronautical Sciences*, Vol. 38, No. 4, 1990, pp. 441–472.

[35]Schulz, V. H., Bock, H. G., and Longman, R. W., "Optimal Path Planning for Satellite Mounted Robot Manipulators," *Advances in the Astronautical Sciences*, Vol. 82, pt. 1, edited by R. G. Melton, L. J. Wood, R. C. Thompson, and S. J. Kerridge, American Astronautical Society, Springfield, VA, 1993, pp. 311–329.

[36]Schulz, V. H., Bock, H. G., and Longman, R. W., "Shortest Paths for Satellite Mounted Robots," *Computational Optimal Control*, Vol. 115, International Series on Numerical Mathematics, Birkhauser, Basel, Switzerland, 1994, pp. 357–366.

[37]Zhu, W. H., Xi, Y. G., Zhang, Z. J., Bien, Z., and De Schutter, J., "Virtual Decomposition Based Control for Generalized High Dimensional Robotic Systems with Complicated Structure," *IEEE Transactions on Robotics and Automation*, Vol. RA-13, No. 3, 1997, pp. 411–436.